THE ASTROPHYSICAL JOURNAL, 183:711–730, 1973 August 1

THE REDSHIFT-DISTANCE RELATION. V. GALAXY COLORS AS FUNCTIONS OF GALACTIC LATITUDE AND REDSHIFT: OBSERVED COLORS COMPARED WITH PREDICTED DISTRIBUTIONS FOR VARIOUS WORLD MODELS

ALLAN SANDAGE
Hale Observatories, Carnegie Institution of Washington,
California Institute of Technology
Received 1973 January 29; revised 1973 March 19

ABSTRACT

New *BVR* photometry is listed for the brightest several members of clusters of galaxies, for all HMS groups, and for E galaxies that are identified with radio sources. Measurements are given for a set of 72 stars that define the S20 (FW 130) $V - R$ system used here.

The galaxy colors, corrected for K reddening, correlate with galactic latitude and provide a new solution for galactic reddening. A model for galactic absorption similar to that proposed by McClure and Crawford is supported. The reddening variation with galactic latitude is smaller by a factor of 2 than traditional values.

Redshifts of E galaxies in the range $0 < z < 0.9$ can be uniquely determined by a combination of four broad-band colors alone near effective wavelengths of B, V, R, and $\langle\lambda\rangle = 8500$ Å. The color-redshift relations are tight, and agree with predicted distributions obtained by redshifting a standard spectrum through the measuring bands. The data admit color evolution for E and S0 galaxies at rates that must be smaller than $\Delta(B - V)/\Delta \log t \simeq 0.3$ mag color change between ages of 10^9 and 10^{10} years, i.e., 0.3 mag dex^{-1}. This observational limit agrees with the color-decay rates that are expected to lie between 0.3 and 0.1 mag dex^{-1} from empirical considerations of C-M diagrams. Although small, such rates are large enough to encourage an observational search for color evolution in E galaxies where the look-back time is significantly long ($z > 0.4$).

Color distributions are calculated for various models for the production of galaxies as a function of time. Comparison with the observed distribution shows that (1) there are no young ($t \leq 10^9$ years) E galaxies in our sample, and (2) the formation epoch for E galaxies was peaked toward the old age side of the distribution. The data are consistent with the view that E galaxies formed at some definite time in the past. Continuous E galaxy formation, as required in the steady-state model, is not verified here. The data do not contradict the hypothesis that giant E galaxies are the same age as the elliptical galaxy component of the Local Group ($t \simeq 10^{10}$ years).

Subject headings: cosmology — galaxies, photometry of — interstellar reddening — redshifts

I. INTRODUCTION

The energy distribution (per unit wavelength) for elliptical and S0 galaxies is a steeply rising function from λ_0 3300 Å to λ_0 4500 Å, after which it flattens redward (Oke and Sandage 1968; Whitford 1971; Schild and Oke 1971). Because of this, photometry of galaxies with redshifts in the interval $0 \leq z \lesssim 0.4$ will show the smallest effects of the spectrum shift (K dimming) if the effective wavelength of the detector is put longward of $\lambda_0 \simeq 6500$ Å.

Beginning in 1960, the commercial availability of multialkali S20 or S25 photomultipliers with their extended red response made possible routine observations of $V - R$ colors (Sandage and Smith 1963; Mendoza 1967) where the effective wavelength of R is $\langle\lambda\rangle \simeq 6700$ Å. Such photomultipliers (ITT-FW 130) were put into routine use at both Mount Wilson and Palomar in 1967. Observations of galaxies in clusters, in groups, and identified as radio sources were begun with the new equipment in that year to supplement similar data obtained earlier with 1P21-S4 photomultipliers (Sandage 1972*c*, *d*, hereafter called Papers II and III).

The goals were fourfold. (1) The red observations, with their long baseline in $B - R$, give good leverage for the color-redshift relation (Whitford 1954). The extended baseline should permit a close upper limit to be put on the color evolution in the look-back time. (2) The Hubble diagram in R magnitudes should be well defined because the K_R correction for redshift is scarcely more than the precisely known bandwidth term $2.5 \log (1 + z)$ for the interval $0 < z < 0.2$; the spectrum is nearly flat redward of λ_0 5600 Å. (3) Independent photometry from that reported in Papers II and III permits an estimate of the external errors of the earlier material. Comparison gives some basis to judge the confidence on solutions for q_0 from the reliability of the photometric data alone. (4) Extend the discussion of Paper II on the richness correction by observing brightest E and S0 galaxies in the small groups listed by Humason, Mayall, and Sandage (1956 [hereafter called HMS], table 11).

This fourfold program is the subject of this and the next two papers. In this report we set out the S20 photometric system in § II, list the observed data on galaxies in § III, and discuss information obtained from the color data alone in §§ IV–VII. Reddening due to the galactic system is rederived in § IV; the color-redshift relations and the conditions to be met by a four-color system that will uniquely determine redshifts in the range $0 < z \leq 0.9$ are set out in § V; observational limits on the permitted color evolution in the look-back time are given in § VI; and predictions of color distributions for several world models are compared with the observations in § VII.

II. THE PHOTOMETRIC SYSTEM

The photometry was done with the same filters used previously (Sandage and Smith 1963), including the $CuSO_4$ liquid cell for red-leak suppression in U and B. The R filter was unblocked on the red side. Although tight transformations of $V - r$ to the standard $V - R$ system were obtained, it will be prudent in the future to define the longward response of the R system with a filter, rather than by the cathode itself.

All data in this paper, and those parts of the data that pertain to the S20 photometry in Papers VI, VII, and VIII, are on a system defined by stars listed in table 1. These were used as night-to-night standards for the 100-inch (254-cm) and 200-inch (508-cm) reflectors. The system was carried progressively around the sky, and was closed upon itself between 1967 June and 1968 April.

The listed $(V - R)_{20}$ colors are not on the $(V - r)_{SS}$ system of Sandage and Smith, but are, in the mean, on the system of Mendoza (1967) as determined from our overlap in M67. In turn, Mendoza's system $(V - R)_M$ is reported to be that of the alphabet photometry of Iriarte *et al.* (1965) and of Johnson *et al.* (1966). With as many data for bright stars as are now measured therein, and with a difference only of definition via a color equation between $(V - r)_{SS}$ and $(V - R)_M$, it clearly serves no purpose to maintain separate systems that have the same information content. We therefore choose to transform our data to the Mendoza system. The approximate transformation is $(V - R)_{20} = 0.94(V - r)_{SS} + 0.04$, where $(V - R)_{20}$ is the color listed in table 1, and $(V - r)_{SS}$ is the system of Sandage and Smith.

UBV values, obtained from 1P21 photometry, are known for many stars in table 1. A number have a long photometric history because they have been used as secondary standards (unpublished) with the 20-, 60-, 100-, and 200-inch Hale telescopes between 1954 and 1967, as tied to the fundamental standards of Johnson and Morgan (1953, table 3), and Johnson and Harris (1954, table 1). The V_{20}, and $(B - V)_{20}$ values in table 1 are close approximations to these S4 *UBV* data, and there are no systematic differences from table 1 taken as a whole. However, any individual star listed there

1973ApJ...183..711S

TABLE 1

STARS THAT DEFINE THE S20 PHOTOMETRIC SYSTEM FOR DATA IN TABLES 2, 3, AND 4

Object	α (1950)	δ (1950)	V_{20}	$(U-B)_{20}$	$(B-V)_{20}$	$(V-R)_{20}$	n_{100}	n_{200}	Chart	Remarks
Field Stars										
+30° 50.......	0 20 42	+31 03.7	10.18	1.29	1.23	0.95	3	0	...	Peterson std.
F22..........	2 27 42	+ 5 03	12.74	-0.84	-0.06	-0.07	1	2	1	
F24..........	2 32 30	+ 3 31	12.37	-1.20	-0.22	0.21	1	0	1	
G5-28........	3 15 41	+15 02.3	15.46	0.42	1.33	1.41	0	1	3	
+30° 663......	4 22 40	+30 15.9	10.29	0.27	0.53	0.47	1	0	...	Peterson std.
+30° 1705.....	8 21 24	+30 16.7	9.98	0.24	0.71	0.64	1	0	...	Peterson std.
F34..........	10 36 42	+43 21	11.23	-1.36	-0.30	-0.08	1	0	1	
F81..........	13 29 24	+15 56	13.48	-1.00	-0.20	-0.06	0	2	1	
F84..........	13 32 48	+13 43	11.84	-0.74	-0.17	0.00	0	2	1	
F96..........	14 28 00	+21 30	13.10	0.08	0.07	0.16	0	2	1	
F97..........	14 33 48	+30 20	12.35	-0.04	0.07	0.13	1	0	1	
F98..........	14 36 12	+27 43	11.82	-0.21	0.00	0.07	1	0	1	
F105.........	14 53 06	+12 57	13.01	-0.05	0.01	0.03	1	0	1	
+30° 2726.....	15 55 17	+29 55.1	10.03	0.64	0.89	0.74	1	0	...	Peterson std.
Wolf 672A	17 16 05	+ 2 00	14.35	-0.57	0.11	0.11	0	1	2, 3	G19-20
Wolf 672B	17 16 06	+ 2 00	14.00	1.15	1.53	1.51	0	1	2, 3	G19-21
+30° 3075.....	17 50 45	+30 07.1	10.00	1.56	1.33	1.02	2	0	...	Peterson std.
+26° 3578.....	19 30 24	+26 15	9.31	-0.17	0.42	0.38	1	0	...	In SS list
L997-21......	19 54 00	- 1 09	13.66	-0.59	0.29	0.32	0	1	2	
+28° 3590.....	20 00 12	+28 31.5	10.10	-0.20	0.12	0.18	2	0	...	Peterson std.
+5° 4481......	20 17 54	+ 5 53	10.11	-0.03	0.61	0.58	7	0	...	In SS list
W12754.......	20 22 36	+24 54	10.79	-0.25	0.40	0.43	6	0	...	In SS list
Wolf 1346.....	20 32 13	+24 54	11.47	-0.86	-0.08	-0.13	1	0	2, 3	G186-31
LDS 749B.....	21 29 37	0 00	14.70	-1.00	-0.02	0.10	1	0	2, 3	G26-9
L930-80......	21 44 54	- 7 58	14.75	-0.99	-0.07	0.03	1	2	2	
+28° 4211.....	21 47 00	+28 27	10.53	-1.26	-0.34	-0.14	1	0	...	S4 UBV values
G93-48.......	21 49 53	+ 2 09.4	12.71	-0.75	-0.02	-0.06	3	2	3	
+30° 4564.....	21 54 59	+30 15.3	10.29	0.20	0.68	0.59	1	0	...	
G18-39.......	22 16 06	+ 8 11.7	10.36	-0.20	0.48	0.51	3	0	3	
G67-23.......	22 46 39	+22 20.5	14.34	-0.68	0.21	0.14	1	3	3	
-15° 6290.....	22 50 36	-14 31	10.16	+1.15	+1.60	1.46	1	0	...	S4 UBV values (JM)
+38° 4955.....	23 11 18	+39 09	11.00	-0.11	0.70	0.63	3	0	...	
F108.........	23 13 36	- 2 07	12.96	-1.08	-0.24	-0.05	0	2	1	
G29-38.......	23 26 16	+ 4 58.5	13.02	-0.57	0.17	0.08	0	1	3	
Stars in Clusters or Regions										
3C48A........	1 34 48	+32 54	10.95	0.14	0.58	0.53	1	0	4	
B........	"	"	13.52	-0.01	0.50	0.48	1	5	"	
C........	"	"	13.59	0.05	0.50	0.52	1	0	"	
C^1.......	"	"	12.89	0.14	0.54	0.49	3	4	"	
D........	"	"	14.56	0.05	0.66	0.60	3	5	"	
M67-81.......	8 48 27	+12 00	10.04	-0.42	-0.06	0.02	10	0	5	
83.......	"	"	13.20	0.10	0.60	0.55	3	3	"	
84.......	"	"	10.54	0.97	1.10	0.82	4	0	"	
105.......	"	"	10.31	1.26	1.25	0.95	7	0	"	
108.......	"	"	9.68	...	1.37	1.06	1	0	"	
131.......	"	"	11.21	0.05	0.42	0.43	3	0	"	
136.......	"	"	11.31	0.18	0.64	0.57	4	0	"	
141.......	"	"	10.49	0.99	1.10	0.84	1	0	"	
151.......	"	"	10.55	...	1.10	0.84	1	0	"	
156.......	"	"	10.96	-0.01	0.11	0.14	3	0	"	
157.......	"	"	12.78	0.11	0.60	0.52	2	0	"	
193.......	"	"	12.28	0.76	0.99	0.79	1	0	"	
231.......	"	"	11.49	0.87	1.06	0.78	1	0	"	
M67-III-34....	"	"	11.26	0.96	1.08	0.81	1	1	6	
III-35....	"	"	12.14	0.78	1.01	0.78	1	2	6	
III-53....	"	"	12.51	0.18	0.67	0.57	1	1	6	
3C273B*......	12 26 36	+ 2 20	14.92	1.02	1.10	0.98	4	2	4	
E.......	"	"	12.71	0.13	0.69	0.61	4	1	"	
G.......	"	"	13.51	0.10	0.63	0.55	6	2	"	
M3-III-9......	13 39 54	+28 38	15.63	0.00	0.47	0.54	1	0	7	
193......	"	"	14.74	0.37	0.89	0.77	0	1	"	
216......	"	"	14.04	0.62	1.01	0.86	0	1	"	
297......	"	"	12.89	1.40	1.41	1.06	1	2	"	
1397......	"	"	12.75	(1.63)	1.58	1.16	4	2	"	U-B is 1P21 value
1402......	"	"	12.69	0.12	0.65	0.56	4	2	"	
M92-III-13....	17 15 36	+43 12	12.20:	1.13	1.35	1.06	0	2	8	Variable?
IV-17....	"	"	15.56	0.00	0.03	0.12	0	2	"	
IV-114...	"	"	13.90	0.38	0.88	0.78	0	2	"	
NGC 7790-C ..	23 55 56	+60 57	12.49	0.19	0.55	0.51	0	5	9	
E ..	"	"	12.75	-0.11	0.40	0.44	0	1	"	
J ..	"	"	13.23	0.34	0.53	0.47	0	3	"	
K ..	"	"	13.25	1.28	1.48	1.14	0	1	"	
I ..	"	"	13.16	0.79	1.22	0.99	0	5	"	

Chart References to Table 1:

1. Feige, J. 1959.
2. Luyten, W. J. 1949.
3. Lowell Obs. Bull., Vol. 4, 136; Vol. 6, 233.
4. Penston, M. J. et al. 1971.
5. Johnson, H. L., and Sandage, A. 1955.
6. Eggen, O. J., and Sandage, A. 1964.
7. Sandage, A. 1953; 1970 (Fig. 1).
8. Sandage, A., and Walker, M. F. 1966.
9. Sandage A. 1958.

should not be used alone as a secondary standard for *UBV*, because of the few observations per star in the present S20 system.

It is noteworthy that for the galaxies themselves, the S20 photometry is in systematic agreement to within 0.02 mag of the S4 system of Papers II and III (see § V here, and Paper VI that follows).

III. THE PHOTOMETRIC DATA

Three photometric programs were carried simultaneously.

a) New data were obtained for the brightest several galaxies in the clusters listed in Paper II and for the added clusters Abell 98, 119, 274, 1213, 2029, and 2670. The last two contain good examples of "cD" galaxies; they are illustrated in Matthews, Morgan, and Schmidt (1964), and are important for the calibration of absolute magnitudes of cluster members as a function of Bautz-Morgan (1970) cluster class (Paper VII that follows).

The photometric data are set out in table 2. The brighter galaxies were measured generally at Mount Wilson with the Hooker reflector, while the faint galaxies of large redshift were measured at Palomar with the Hale telescope. Pulse counting was used throughout, with data-readout using equipment built by the Astroelectronics Laboratory. The observations were made through a number of aperture sizes whose diameters are listed in the table.

b) Photometry was obtained for the brighter galaxies in all the E and S0 groups listed by HMS (their table 11) to test for a dependence of absolute magnitude of first-ranked galaxies on the richness of aggregates. The data, set out in table 3, were obtained largely with the 100-inch on Mount Wilson in 1967–1968. The galaxies in these HMS groups are all nearby, bright, and very large, requiring large apertures for adequate aperture corrections by the method of Paper I (Sandage 1972*a*). Because low-speed (5 MHz) pulse amplifiers were then in use, appreciable coin idence corrections were required at the larger apertures, making the subtraction of two large numbers (galaxy plus sky count minus sky count alone) relatively inaccurate. Errors that amount to 0.1 mag in the intensities may be present for apertures larger than $\sim 60''$ diameter in table 3, but data for the smaller apertures will be more accurate. The colors will be affected to a lesser degree. Color values for the largest apertures, where the coincidence corrections are particularly uncertain, are omitted from the table.

c) Many of the radio sources measured in Paper III were remeasured in the present S20 program, and the data are listed in table 4. Tabulated in the "Remarks" column is an estimate of the emission line strength S_6 (defined by Schmidt 1965) as an aid to judge how much the measured colors are affected by line emission. The words *yes* and *no*, based on the size of S_6, or on other knowledge of the spectrum, indicate that the colors were, or were not, used to determine the latitude and redshift effects of §§ IV and V.

IV. SOLUTION FOR GALACTIC REDDENING: NEW ABSORPTION CORRECTIONS

Cosmological information is contained in the data through the correlation of color and redshift. Of principal interest is the second-order color change due to evolution of the stellar content in the look-back time. This is known to be very small. Extraneous color effects must first be removed before there is hope even of its detection.

Galactic reddening is the primary correction. Recent studies have shown that the reddening at high latitudes is exceptionally small, in contrast to the pronounced latitude effect that is usually inferred from the galaxy counts (Hubble 1934; Shane and Wirtanen 1954, 1967; Noonan 1971). Hubble's half-thickness absorption of $A_B \simeq 0.25$ mag, and Shane and Wirtanen's largest values of $A_B \simeq 0.5$ mag, bracket the values by Noonan, de Vaucouleurs and Malik (1969), and others. But *all* are much

TABLE 2

S20 PHOTOMETRY OF BRIGHT GALAXIES IN CLUSTERS

Cluster	z	Tel	Aperture	*V*	*B−V*	*V−R*	Remarks
Virgo........	0.00381	100	24″0	11.18	1.02	0.86	U−B = 0.64
NGC 4486			37.6	10.71	1.02	0.86	U−B = 0.58
b = +70			55.1	10.27	1.05	0.83	U−B = 0.57
			82.2	9.81	...	0.78	U−B = 0.62
Peg I........	0.01279	100	20.0	12.79	1.10	0.91	
2317 + 0755			35.2	12.38	1.09	0.91	NGC 7619
b = -48			64.0	12.04	1.05	0.96	
0122 + 3305...	0.0170	100	37.6	12.68	1.06	0.86	
b = -29			55.1	12.38	1.05	0.86	NGC 507
			82.2	12.09	...	0.89	
			119.0	11.91	...	...	
Perseus......	0.01811	100	11.4	13.48	0.70	0.86	U−B = −0.16
NGC 1275			37.6	12.51	...	0.90	
b = -13							
Abell 1213....	0.0287	100	24.0	14.50	1.07	0.87	N1
b = +69			37.6	14.22	1.11	0.79	
			24.0	14.41	1.13	0.90	N2
			37.6	14.28	1.07	0.86	
			24.0	14.81	1.23	0.81	N3
Abell 119.....	0.0387	200	12.2	14.79	1.11	0.89	
b = -64			18.8	14.48	1.10	0.90	N2
			30.6	14.21	1.12	0.90	
			12.2	15.05	1.16	0.88	
			18.8	14.63	1.15	0.89	N1
			30.6	14.24	1.13	0.84	
Peg II	0.0428	100	20.0	14.49	1.17	0.91	NGC 7503
2308 + 0720			35.2	14.26	1.21	0.95	
b = -48							
2322 + 1425...	0.0439	100	20.0	(14.97)	1.20	0.92	
NGC 7649			35.2	(14.60)	1.20	0.92	
b = -43		200	18.8	14.86	1.10	0.92	
			30.6	14.42	1.13	0.93	
			48.3	13.91	1.10	0.89	Includes star
			7.6	16.49	0.87	0.73	Star alone
		200	12.2	15.51	1.11	0.92	
			18.8	15.24	1.08	0.94	N7
		100	20.0	15.31	...	0.91	
		200	18.8	15.49	1.10	0.92	N1
			30.6	15.32	1.05	0.91	
0106 - 1536...	0.0526	200	30.6	14.08	1.12	0.90	N1 + N2
Haufen A			48.3	13.83	1.15	0.90	of HMS
b = -78							
			12.2	15.49	1.19	0.90	N10
			12.2	15.12	1.14	0.89	N2?
1239 + 1852...	0.0718	100	15.2	15.19	1.19	0.94	
Abell 1589			24.0	14.88	1.18	0.92	
Virgo 2			24.0	14.84	1.26	0.93	N4
b = +81			37.6	14.59	1.20	0.86	
			37.6	14.61	1.32	0.93	
			24.0	15.17	1.21	0.98	N2
			24.0	15.20	1.28	0.86	N1
			37.6	15.17	1.34	0.96	
1520 + 2754...	0.0722	100	24.0	15.62	1.17	0.93	
Cor Bor			24.0	15.57	1.20	0.98	N2
b = +57			37.6	15.47	(1.47)	0.94	
			37.6	15.42	(1.45)	0.96	
			24.0	16.04	1.10	0.92	N3
			24.0	16.29	...	...	
Abell 2670 ...	0.07745	200	12.2	15.57	1.26	0.91	
b = -69			18.8	15.25	1.25	0.92	N1
			30.6	14.88	1.16	0.94	
			12.2	16.42	1.29	0.92	NA
			18.8	16.30	1.27	0.92	
Abell 2029 ...	0.0777	100	24.0	14.44	1.27	0.89	
b = +50			37.6	14.17	1.19	0.95	
0705 + 3506...	0.0779	200	12.2	15.74	1.31	0.94	N1
Gemini			18.8	15.42	1.28	0.89	
b = +18			18.8	15.96	1.15	1.00	N2
			30.6	15.68	1.23	0.87	
			12.2	16.22	1.30	0.94	
			18.8	15.96	1.20	0.93	N1A
			30.6	14.89	1.28	0.94	
1513 + 0433...	0.0944	100	24.0	15.79	1.28	0.92	N1
b = +49			37.6	15.56	1.22	0.89	
Abell 98......	0.10282	200	12.2	16.29	1.39	0.98	
b = -42			18.8	15.99	1.32	0.96	NA
			30.6	15.67	1.32	0.97	
			12.2	16.63	1.36	0.97	NE
			18.8	16.36	1.39	1.01	
			12.2	16.33	1.36	1.02	N1
			18.8	16.09	1.38	1.03	
Abell 274.....	0.12890	200	12.2	16.67	1.45	1.01	N1
b = -64			18.8	16.38	1.40	0.99	
			12.2	16.88	1.05	0.90	NA
			18.8	16.60	1.03	0.82	
			12.2	16.95	1.43	0.97	NE
			18.8	16.68	1.47	0.98	
Abell 2224....	(0.14993)	200	18.8	17.13	1.58	...	N2
b = +34							
			12.2	17.50	1.19	...	N1
			18.8	17.50	1.13	...	
0025 + 2223...	0.1594	200	12.2	17.32	1.50	0.98	N4
b = -40			18.8	17.08	1.47	0.96	
			12.2	17.64	1.56	0.96	N2
			18.8	17.45	1.45	1.05	
			12.2	17.84	1.55	1.01	N1
			18.8	17.77	1.46	1.01	
0138 + 1832...	0.1730	200	12.2	18.17	1.55	1.04	N1
b = -43			18.8	17.81	1.59	0.99	
			?	18.46	1.58	1.09	ND
0925 + 2044...	0.1917	200	12.2	17.10	1.57	1.13	N1 + N1A
b = + 43			18.8	16.82	1.56	1.09	
0855 + 0327...	0.2018	200	12.2	17.21	1.65	1.09	N8+N9
Hydra			18.8	16.92	1.50	1.15	+ N9A
b = +29							
			12.2	17.89	1.68	1.03	N1
			18.8	17.72	1.89	1.10	
1447 + 2617...	0.36						
N4		200	12.2	19.93	1.49	1.60	
N3		200	12.2	20.17	1.21	1.49	
b = +63							
3C295........	0.461	200	7.6	19.74	1.46	1.64	
N1			12.2	19.56	1.38	1.83	
b = +61							
Abell 2204....	...	200	12.2	16.59	1.20	...	
b = +33			18.8	16.09	1.30	...	
Abell 2652....	...	200	12.2	17.47	0.81	0.61	NE
b = -67			12.2	17.70	0.48	0.58	NB
			12.2	18.50	1.56	1.01	NC
3C31.........	0.01755	100	20.0	13.37	1.11	0.91	HMS group
NGC 383			35.2	13.01	1.08	0.90	
b = -30							
3C40.........	0.0180	100	20.0	13.63	1.05	0.89	NGC 545
NGC 545/7			35.2	13.15	1.04	0.89	
b = -63							
			20.0	13.57	1.08	0.89	NGC 547
			35.2	13.14	1.06	0.89	
3C66.........	0.0215	100	24.0	13.77	1.07	0.93	N1
b = -17			37.6	13.16	0.94	0.86	N1 + star
			15.2	14.92	1.06	0.78	Star alone
			37.6	13.40	0.91	0.87	N1 alone by cal.
3C465........	0.0301	100	15.2	14.28	1.15	0.91	N1 alone
NGC 7720			15.2	14.95	1.02	0.93	N2 alone
b = -33			55.1	13.10	1.07	0.88	N1 + N2
			82.2	13.01	1.01	1.03	N1 + N2
		200	12.2	14.39	1.13	0.96	N1
			18.8	13.99	1.12	0.94	N1
			12.2	15.13	1.07	0.92	N2 alone
			48.3	13.26	1.11	0.94	N1 + N2
3C338........	0.0303	100	37.6	13.05	1.08	0.82	
NGC 6166			55.1	12.78	1.06	0.83	
Abell 2199			82.2	12.59	1.04	0.88	
b = 44							
3C317........	0.0351	100	37.6	13.90	1.08	0.94	
Abell 2052			55.1	13.53	1.13	0.90	
b = +50							
M23 - 112	0.0825	200	12.2	16.22	1.05	0.95	
b = -64			18.8	15.81	1.10	0.92	
			30.6	15.57	1.01	0.94	
3C219........	0.1745	200	12.2	17.44	1.38	0.94	
b = 45							
3C28.........	0.1959	200	12.2	17.89	1.30	1.17	
Abell 115			12.2	17.82	1.44	1.10	
b = -37			18.8	17.59	1.41	1.16	
			18.8	17.59	1.50	1.15	

TABLE 3

S20 PHOTOMETRY OF GALAXIES IN GROUPS MOSTLY FROM HMS TABLE XI

Group	Galaxy	Tel	Aper.	V	B–V	V–R	U–B	Remarks
G68..........	NGC 68	100	15".2	14.59	1.08	0.90	...	
z = 0.0226	S0		24.0	14.22	0.98	0.90	...	
b = -32°			24.0	14.13	1.11	0.85	...	
n = 20±			37.6	13.86	1.02	0.83	...	
			55.1	13.52	...	...	...	
	NGC 70		24.0	14.31	1.08	0.90	...	
	NGC 71		24.0	14.23	1.00	0.87	...	
	E2		37.6	13.88	1.01	0.85	...	
G80..........	NGC 80	100	24.0	13.43	1.12	0.86	...	
z = 0.0209	S0		37.6	13.10	1.08	0.88	...	
b = -40°			55.1	12.82	1.06	0.88	...	
n = 12			82.2	12.66	...	...	...	
	NGC 83		37.6	13.33	1.19	0.90	...	
	E0			13.10	(1.09)	0.93	...	
G128.........	NGC 128	100	37.6	12.50	...	0.84	...	
z = 0.0155	S0		55.1	12.18	1.01	0.84	...	
b = -60°			82.2	12.07	0.91	0.91	...	
n = 5	NGC 125		37.6	13.25	0.95	0.75	...	
	S0		55.1	13.06	0.88	0.78	...	
G194.........	NGC 194	100	24.0	13.22	1.01	0.85	...	
z = 0.0177	E1		37.6	12.94	0.98	0.82	...	
b = -60°			55.1	12.70	0.92	0.86	...	
n = 10			82.2	12.60	0.92	0.95	...	
	NGC 193		24.0	13.34	1.04	0.85	...	
			37.6	13.00	1.04	0.82	...	
			55.1	12.76	1.06	0.86	...	
	NGC 198		37.6	13.37	0.77	0.75	...	
			55.1	13.02	0.69	0.75	...	
G383.........	NGC 383	100	20.0	13.37	1.11	0.91	...	
z = 0.0176	S0		35.2	13.01	1.08	0.90	...	
b = -30°	NGC 382		20.0	14.27	...	0.89	...	
n = 12	E0							
3C31								
G507.........	NGC 507	100	37.6	12.68	1.06	0.86	...	
z = 0.0155	E3		55.1	12.38	1.05	0.86	...	
b = -29°			82.2	12.09	0.97	0.89	...	
n = 35±			119.0	11.91	0.97	0.91	...	
Cl 0122+33	NGC 499		37.6	12.81	1.05	0.87	...	
	S0		55.1	12.56	1.05	0.87	...	
			82.2	12.37	1.09	0.88	...	
	NGC 508		37.6	13.68	1.06	0.93	...	
			55.1	13.38	1.06	0.86	...	
	NGC 496		37.6	14.43	0.69	0.81	...	
G547.........	NGC 547	100	20.0	13.57	1.08	0.89	...	
G564			35.2	13.14	1.06	0.89	...	
z = 0.0180	NGC 545		20.0	13.63	1.05	0.89	...	
b = -63°	3C40		35.2	13.15	1.04	0.89	...	
n > 20	NGC 543		20.0	13.87	1.04	0.88	...	
			35.2	13.46	1.09	...	...	
	NGC 564		20.0	13.88	...	0.87	...	
	E3		35.2	13.40	1.02	0.88	...	
G741.........	NGC 741	100	20.0	13.37	1.06	0.91	...	
z = 0.0188	E0		35.2	12.79	1.10	0.85	...	
b = -54°								
n = 9								

Group	Galaxy	Tel	Aper.	V	B–V	V–R	U–B	Remarks
G1600........	NGC 1600	100	20.0	12.94	1.08	0.85	...	
z = 0.0160	E5		35.2	12.39	1.03	0.83	...	
b = -33°			64.0	11.97	1.01	0.89	...	
n = 8			37.6	(12.60)	(0.94)	(0.99)	...	
			55.1	(12.26)	(1.06)	(0.98)	...	
			82.2	12.10	(0.95)	(1.02)	...	
G2563........	NGC 2563	100	37.6	12.97	1.06	0.89	...	
z = 0.0159	S0		37.6	13.01	1.07	0.92	...	
b = +29°			55.1	12.78	1.06	0.91	...	
n = 20			55.1	12.81	1.00	0.96	...	
			82.2	12.51	1.04	0.83	...	
			82.2	12.56	1.10	0.84	...	
	NGC 2562		37.6	13.23	1.06	0.90	...	
	Sa		55.1	13.16	0.95	0.95	...	
G2832........	NGC 2832	100"	24.0	13.15	1.06	0.89	0.73	
z = 0.0200	E2		24.0	13.17	1.09	0.87	...	
b = +44°			37.6	12.85	1.02	0.90	0.60	
n = 30±			37.6	12.85	1.02	0.90	0.60	
	+2831		82.2	12.23	1.05	0.83	...	
	E1		82.2	12.26	1.06	0.84	...	
Δmag (tot)	{NGC 2831		24.0	14.03	1.03	0.86	0.65	
= 2.23	alone}		24.0	14.12	1.01	0.87	...	
	NGC 2839		37.6	14.17	0.99	...	...	
G3158........	NGC 3158		24.0	13.09	1.07	0.87	...	
z = 0.02336	E3		37.6	12.94	0.94	0.96	...	
b = +55°			55.1	12.63	1.05	0.89	...	
			55.1	12.63	1.01	0.90	...	
n = 20			82.2	12.44	1.02	0.90	...	
			82.2	12.31	1.03	(0.79)	...	
		P60	50.0	12.70	1.04	...	0.63	
			71.8	12.45	1.08	...	0.58	
			103.5	12.27	1.06	...	0.57	
	NGC 3159	100	24.0	14.10	1.01	0.87	...	
	E3		37.6	13.96	0.88 ?	0.87	...	
			37.6	13.93	0.98	0.84	...	
			55.1	13.81	0.99	0.91	...	
			55.1	13.82	1.01	0.87	...	
	NGC 3163	100	24.0	13.84	1.05	0.85	...	
			37.6	13.75	...	1.01	...	
			37.6	13.54	0.96	0.88	...	Plus star
			55.1	13.41	0.97	0.88	...	Plus star
			15.2	16.43	0.21	1.03	...	Star alone
			{37.6	13.64	1.04	0.87	...}	NGC 3163
			55.1	13.50	1.04	0.87	...	alone
G3190........	NGC 3193	100	37.6	11.88	0.97	0.85	0.55	
z = 0.00399	E2		55.1	11.66	0.94	0.86	0.48	
b = +55°			82.2	11.36	1.03	(0.77)	...	
n = 5			119.0	10.98	...	...	...	
	NGC 3190	100	55.1	11.60	1.01	0.88	0.49	
	Sa		82.2	11.36	1.04	0.85	0.49	

TABLE 3 -continued

Group	Galaxy	Tel	Aper.	V	$B-V$	$V-R$	$U-B$	Remarks
Leo G........	NGC 3368	100	15.2	11.91	1.14	0.97	0.66	
z = 0.00263	Sa		24.0	11.42	1.06	0.95	0.64	
b = +64°			37.6	11.03	1.03	(0.90)	0.59	
n = 20±			55.1	10.64	1.03	(0.88)	(0.51)	
			82.2	10.21	1.04	...	(0.51)	
			341.5	(9.86)	(1.03)	...	...	
	NGC 3379	100	37.6	10.76	0.99	0.87	0.69	
	E0		55.1	10.52	0.97	0.88	0.63	
			82.2	10.24	1.02	0.86	0.59	
			119.0	9.92	1.03	0.83	0.64	
	NGC 3623	100	15.2	12.22	1.09	0.95	0.69	
	Sa		55.1	10.70	0.98	0.88	0.60	
			82.2	10.20	1.05	0.83	0.62	Plus star
			15.2	14.14	0.87	0.82	0.72	Star alone
	NGC 3627	100	15.2	11.95	1.02	0.93	0.62	
	Sb		24.0	11.44	0.98	0.92	0.57	
			37.6	11.04	0.95	0.88	0.53	
			55.1	10.64	0.91	0.87	0.41	
			82.2	10.18	0.87	0.81	0.35	
			119.0	9.67	0.89	0.76	0.32	
G5044........	NGC 5044	100	37.6	12.31	1.02	0.90	...	
z = 0.00867			55.1	11.94	1.03	0.88	0.55	
b = +46°			82.2	11.56	...	...	...	
n = 15		P60	71.8	11.70	1.03	...	0.58	
			103.5	11.42	1.03	...	0.60	
			145.9	11.26	1.06	...	0.56	
	NGC 5035	P60	71.8	12.93	0.86	...	0.42	
			103.5	12.92	0.87	...	...	
G5077........	NGC 5077	100	24.0	12.55	1.05	0.91	0.57	
z = 0.00838	E3		55.1	12.02	0.98	0.89	0.51	Plus star
b = +50°			82.2	11.72	1.12	0.80	...	Plus star
n = 8			15.2	14.52	0.73	0.73	0.13	Star alone
		P60	38.0	12.05	1.02	...	0.57	Poor night
			50.0	11.88	1.05	...	0.53	Poor night
			71.8	11.69	1.04	...	0.62	Poor night
			103.5	11.60	1.05	...	0.60	Poor night
		NGC 5077 is of low surface brightness and has a very diffuse image.						
G5371........	NGC 5353	100	55.1	11.55	...	0.88	...	
z = 0.00761			55.1	11.50	1.00	0.88	0.66	
b = +71°			82.2	11.45	1.01	0.90	...	
n = 5			82.2	11.27	...	0.85	0.64	
			119.0	10.99	...	...	...	+N5354
		P60	71.8	11.48	1.02	...	0.59	
			103.5	11.16	1.03	...	0.61	
			145.9	10.77	1.01	...	0.59	
	NGC 5354	100	37.6	12.32	1.00	0.87	...	
	E4		55.1	12.08	0.99	0.86	0.55	
			82.2	11.84	1.02	0.84	...	
		P60	71.8	11.86	0.99	...	0.52	
			103.5	11.55	1.02	...	0.51	
	NGC 5371	100	37.6	12.63	0.98	0.86	0.52	
	Sb		55.1	12.25	0.89	0.86	...	
			82.2	11.79	0.85	0.80	...	
			119.0	11.21	0.82	0.71	...	
		P60	50.0	12.36	0.99	...	0.45	
			71.8	11.93	0.88	...	0.36	
			103.5	11.46	0.83	...	0.25	
			145.9	11.06	0.77	...	0.21	
	NGC 5350	P60	71.8	12.14	0.80	...	0.22	
	Sc		103.5	11.98	0.94	...	0.43	
	NGC 5355	P60	50.0	13.55	0.87	...	0.26	
	E							
G5846........	NGC 5846	100	37.6	11.77	1.02	0.89	0.70	
z = 0.00603	E0		55.1	11.44	1.04	0.90	0.69	
b = +49°			82.2	10.98	1.10	0.85	...	+ 2 stars
n = 10			119.0	10.62	1.10	0.76	...	+ 2 stars
			15.2	13.70	1.04	0.83	...	South star
			15.2	15.24	0.94	0.74	...	North star
			82.2	11.10	1.11	0.86	...	N5846 alone
			119.0	10.71	1.11	0.76	...	N5846 alone
		P60	50.0	11.56	0.98	...	0.67	
			71.8	11.14	1.04	...	0.66	
			103.5	10.77	1.07	...	0.58	+ star
			26.1	13.27	1.02	0.52	...	South star
	NGC 5813	100	55.1	11.80	1.00	0.91	0.59	
	E1		82.2	11.48	1.00	0.88	0.67	
			119.0	10.98	(1.24)	(0.72)	...	
		P60	71.8	11.53	1.03	...	0.62	
			103.5	11.27	1.01	...	0.58	
	NGC 5838	P60	50.0	11.88	(0.83)	...	0.55	Poor night
	S0		71.8	11.46	1.01	...	...	Poor night
			103.5	11.30	1.02	...	0.53	Poor night
			145.9	11.19	0.95	...	0.58	Poor night
	NGC 5831	P60	50.0	12.22	1.03	...	0.50	
	E3		71.8	12.02	1.07	...	0.49	
	NGC 5850	100	55.1	12.41	1.05	0.88	0.60	
	SBb		82.2	12.13	1.07	0.88	...	
G6027........	All six	100	82.2	12.78	0.90	0.84	0.36	
z = 0.01455			119.0	12.60	0.85	0.85	...	
b = +47°	B alone		37.6	14.03	1.01	0.88	...	B alone
n = nest			37.6	13.72	0.86	0.87	...	N6027 + d
	All six	P60	103.5	12.70	0.98	...	0.32	Poor night
			145.9	12.60	0.92	...	...	Poor night
G7242........	NGC 7242	100	24.0	13.87	1.17	0.97	...	
z = 0.02041	E3		37.6	13.40	1.16	0.91	...	
b = −16°			55.1	12.97	1.12	0.93	...	
n = 15	N7242a		24.0	14.93	1.18	...	...	
	S0							
G7385........	NGC 7385	100	20.0	13.81	1.13	0.92	...	
z = 0.02579	E0		35.2	13.39	1.07	0.93	...	
b = -41°	NGC 7386		20.0	13.93	1.17	0.90	...	
n = 13±	S0		35.2	13.60	1.11	0.92	...	
			64.0	13.36	...	0.98	...	
G7619........	NGC 7619	100	20.0	12.79	1.10	0.91	...	
z = 0.01279	E3		35.2	12.38	1.09	0.91	...	
b = -48°			64.0	12.04	1.05	0.96	...	
n = 20±	NGC 7626		20.0	13.01	1.10	0.90	...	
	E1		24.0	12.74	1.07	0.89	...	
			35.2	12.51	1.10	0.89	...	
			37.6	12.35	1.08	0.85	...	
			64.0	12.07	1.01	0.94	...	
			82.2	11.88	0.98	0.93	...	
	NGC 7562		37.6	12.39	1.11	0.87	...	
			55.1	12.19	1.06	0.91	...	
			82.2	12.08	1.08	1.04	...	
VV172........	A	200	12.2	16.56	1.14	0.92	0.62	
z = 0.0526	B		12.2	16.95	0.89	0.76	0.13	
for A, C, D, E	C		12.2	15.57	1.13	0.94	0.48	
z = 0.12293	D		12.2	16.45	1.21	1.01	0.50	
for B	E		12.2	16.02	1.12	0.90	0.49	
b = +45°								
n = 5								

TABLE 4

S20 PHOTOMETRY OF RADIO GALAXIES

Source	z	Tel	Aper.	V	B−V	V−R	U−B	Remarks
3C15	0.0733	100	15.2	15.88	...	0.91	...	Brightest member
b = -64		200	12.2	16.04	1.12	0.89	...	of small group
			18.8	15.80	...	0.89	...	λ3727; H,K abs:
			30.6	15.53	1.18	0.87	...	Yes.
3C17	0.2201	200	7.6	18.20	0.69	0.87	-0.37	Isolated N?
b = -65			12.2	18.00	0.82	0.84	-0.35	S_6 = 7: No.
3C26 .... b = -67	0.2106	200	12.2	18.21	1.14	0.86	...	Isolated: S_6 = 11: No.
3C28	0.1959	200	12.2	17.89	1.30	1.17	...	Brightest member
b = -37			12.2	17.82	1.44	1.10	...	of rich cluster
			18.8	17.59	1.41	1.16	...	A115; S_6 = 2, λ3727:
			18.8	17.59	1.50	1.15	...	No.
3C29	0.0450	200	18.8	14.70	1.11	0.89	...	Outlying member
b = -64			30.6	14.40	1.04	0.91	...	of rich Abell
			48.3	14.14	1.04	0.88	...	cluster A119? S_6=0 Yes.
3C33	0.0600	200	12.2	15.82	1.17	0.82	...	Isolated
b = -49			18.8	15.59	1.14	0.89	+0.37	S_6 = 12. No.
			48.3	15.39	1.18	0.82	...	
3C40	0.0180	100	20.0	13.63	1.05	0.89	...	Companion to
b = -63			35.2	13.15	1.04	0.89	...	NGC 547. In cluster A194. Yes.
3C66	0.0215	100	24.0	13.77	1.07	0.93	...	Alone
b = -17			37.6	13.16	0.94	0.86	...	Plus star
			15.2	14.92	1.06	0.78	...	Star alone. S_6 = ?
3C71	0.0038	200	4.9	11.76	1.03	0.60	-0.02	NGC 1068
b = -52			7.6	11.37	1.02	0.69	+0.02	Seyfert. No.
			12.2	10.95	0.98	0.73	+0.09	
		100	11.4	11.03	0.92	0.78	+0.10	
			15.2	10.82	0.91	0.80	+0.14	
3C75	0.0241	100	15.2	14.58	1.22	1.01	...	North alone
In small			15.2	14.94	1.21	1.05	...	South alone
cluster			55.1	13.34	1.24	0.98	...	North + South
A400.		200	12.2	14.66	1.25	1.06	...	North alone
Dumbell			18.8	14.39	1.24	1.04	...	North alone
b = -45			12.2	15.01	1.22	1.04	...	South alone
			18.8	14.67	1.22	1.04	...	South alone
			48.3	13.52	1.22	1.05	...	North + South S_6 = ? No.
3C76.1	0.0328	200	18.8	15.52	1.13	0.96	...	Isolated
b = -36			30.6	15.33	1.08	0.90	...	S_6 = 0. Yes.
3C78	0.0289	100	24.0	13.72	1.15	0.99	...	NGC 1218
b = -45			37.6	13.46	1.15	0.99	...	Isolated
			55.1	13.16	1.13	0.94	...	$S_6 \simeq$ 1. Yes.
		200	18.8	13.51	1.15	1.00	...	
			30.6	13.89	1.16	1.00	...	
3C83.1 .... b = -13	0.0181	100	37.6	13.80	1.15	0.97	...	NGC 1265 In Per Cl. Yes.
3C84	0.0181	100	11.4	13.48	0.70	0.86	-0.16	NGC 1275
b = -13			37.6	12.51	...	0.90	...	In Per Cl = A426 No.
3C88	0.0302	100	24.0	14.95	...	0.95	...	Isolated
b = -42			37.6	14.48	1.11	0.88	...	S_6 = 2. Yes.
			55.1	14.24	1.08	0.94	...	
		200	18.8	15.06	1.14	0.96	...	
			30.6	14.65	1.13	0.98	...	
			48.3	14.32	1.14	1.00	...	
3C98	0.0306	100	24.0	15.14	1.18	0.97	...	Single, isolated
b = -31			37.6	14.98	1.24	0.93	...	S_6 = 8. No.
			12.2	15.42	1.21	0.98	+0.63	
			18.8	15.21	1.17	0.99	...	
			30.6	14.98	1.21	0.99	...	
3C192	0.0596	200	12.2	16.08	1.23	0.87	...	In small group.
b = +26			18.8	15.83	1.18	0.86	...	λ3737, N1, N2. Yes?
3C198	0.0809	200	12.2	17.05	0.97	0.75	...	In small group?
b = +23			18.8	17.01	0.83	0.83	...	S_6 = 7. No.
3C219 .... b = +45	0.1745	200	12.2	17.44	1.38	0.94	...	In rich cluster. S_6 = 8. No.
3C223.1 ...... b = +49	0.1075	200	18.8	16.56	1.29	0.92	...	Isolated? or Gr? λ3727, N1, N2. No.
3C264	0.0206	100	24.0	13.62	1.05	0.88	0.61	NGC 3862
b = +73			37.6	13.41	1.07	0.89	...	S_6 = 0. Yes.
			55.1	13.20	0.98	0.89	...	
			82.2	13.00	1.00	0.86	...	
3C270	0.0070	100	37.6	11.62	0.96	0.87	0.62	NGC 4261.
b = +67			55.1	11.32	1.00	0.84	0.59	S_6 = 0. Yes.
			82.2	11.02	1.02	0.81	...	
3C272.1	0.0029	100	37.6	10.85	0.99	0.88	0.62	NGC 4374
b = +74			55.1	10.52	1.01	0.85	0.56	Yes?
			82.2	10.17	1.07	0.80	...	
3C278	0.0143	100	24.0	12.73	1.14	0.93	0.66	NGC 4782 is
NGC 4782			37.6	12.40	1.04	0.91	...	radio source. Dumbell
b = +50			82.2	11.40	1.11	0.80	...	Plus 2 stars
			15.2	15.57	0.63	0.68	...	West star
			15.2	16.06	1.09	0.65	...	East star S_6 = 0. Yes.
3C278a	0.0143	100	37.6	12.69	1.02	0.86	0.67	NGC 4783
b = +50			55.1	12.36	1.00	0.87	...	
3C293	0.0454	100	55.1	14.34	0.96	0.75	...	Isolated
b = +76			82.2	14.29	1.04	0.88	...	λ3727. Yes.
3C296	0.0237	100	37.6	12.75	1.04	0.88	0.71	Ic 5532
b = +62			55.1	12.51	1.08	0.85	...	S_6 = 0. Yes.
			82.2	12.24	1.02	0.87	...	
			119.0	11.96	1.17	0.79	...	
			24.0	14.34	1.00	0.84	...	Companion 35" south
3C317 #1	0.0351	100	37.6	13.90	1.08	0.94	...	In cluster A2052.
b = +50			55.1	13.53	1.13	0.90	...	S_6 = 3. Yes.
3C318.1	0.0440	200	12.2	15.46	1.13	0.98	0.58	In group. S_6 = 0.
G1			18.8	15.03	1.12	0.95	0.56	Yes.
b = +49			30.6	14.67	1.11	0.94	...	
		P60	50.0	14.24	1.15	...	...	
			71.8	14.03	1.10	...	...	
3C318.1	0.0475	200	18.8	15.47	1.14	0.96	0.49	S_6 = 0. Yes.
G2			30.6		1.10	0.92	...	
b = +49		P60	50.0	15.20	1.21			
3C338	0.0303	100	37.6	13.05	1.08	0.82	0.61	NGC 6166 in
b = +44			55.1	12.78	1.06	0.83	0.56	Abell 2199
			82.2	12.59	1.04	0.88	...	S_6 = 0. Yes.
3C381	0.1614	200	7.6	17.99	1.45	0.89	...	Brightest in small
b = +23			12.2	17.66	1.39	0.96	...	group. Five em lines. No.
3C382	0.0586	200	12.2	15.39	1.14	0.92	...	Isolated
b = +17			18.8	15.16	1.15	0.93	...	S_6 = 5. No.
			30.6	15.01	1.14	0.94	...	
3C388	0.0917	200	7.6	16.52	1.42	0.94	...	N1 S_6 = 1.
b = +20			12.2	16.04	1.31	0.98	...	N1 Yes.
			7.6	17.31	1.46	1.00	...	N2
			30.6	15.23	1.40	0.98	...	N1 + N2
3C402	0.0255	200	18.8	14.40	1.19	1.01	0.73	S_6 = 0. Yes.
G3			30.6	14.13	1.15	1.02	...	
b = +13		P60	50.0	14.05	1.23	...	...	
3C402	0.0263	P60	38.0	13.38	1.14	...	...	S_6 = 0. Yes.
G1			38.0	13.56	0.94	...	...	
b = +13			50.0	13.20	1.15	...	...	
			50.0	13.23	1.10	...	0.76	
			71.8	13.03	1.13	...	...	
3C436 .... b = -19	0.2154	200	12.2	18.28	1.45	1.17	...	S_6 = 5. No.
3C442	0.0270	100	24.0	14.60	1.09	0.93	...	In an extended
NGC 7237			37.6	14.21	0.91	0.87	...	group or cluster.
b = -34			55.1	13.71	1.20	0.76	...	$S_6 \simeq$ 1. Yes.
Near 3C442	0.0270	100	24.0	14.18	1.08	0.89	...	NGC 7236
b = -34			37.6	13.89	1.04	0.81	...	
3C449	0.0181	100	24.0	14.06	1.13	0.93	...	Brightest in
b = -16			37.6	13.81	1.16	0.88	...	small group.
			55.1	13.66	1.00	0.96	...	S_6 = 0. Yes.
3C452	0.0820	200	7.6	16.99	1.37	0.96	...	Probably in a
b = -17			12.2	16.55	1.22	0.89	...	cluster or group. S_6 = 5. No.
3C455	0.0331	100	15.2	14.94	1.08	0.88	0.29	Isolated.
b = -41			24.0	14.70	1.00	0.91	...	S_6 = 0. Yes.
			37.6	14.39	1.09	0.81	...	
3C456	0.2337	200	7.6	18.99	0.70	1.10	...	S_6 = 7. No.
b = -46			12.2	18.85	0.88	1.17	...	
MSH 23-112...	0.0825	200	12.2	16.22	1.05	0.95	...	S_6 = 7. No.
b = -64			18.8	15.81	1.10	0.92	...	
			30.6	15.57	1.01	0.94	...	
3C465	0.0301	200	12.2	14.39	1.13	0.96	...	N1 alone. S_6 = 1.
NGC 7720			18.8	13.99	1.12	0.94	...	N1 alone. Yes.
Abell 2634			12.2	15.13	1.07	0.92	...	N2 alone.
b = -33			48.3	13.26	1.11	0.94	...	N1 + N2.
		100	15.2	14.28	1.15	0.91	...	N1 alone.
			15.2	14.95	1.02	0.93	...	N2 alone.
			55.1	13.10	1.07	0.88	...	N1 + N2.
			82.2	13.01	1.01	(1.03)	...	N1 + N2.
		200	12.2	15.32	1.11	0.93	0.64	NB
			18.8	14.88	1.09	0.92	...	NC

larger than would be predicted from the observed polar cap reddening from many recent determinations (summarized in Paper II, § III*b*, with references).

In view of the problem, we have made yet another solution for systematic reddening as a function of galactic latitude from the new color data in tables 2, 3, and 4. Mean $B - V$, $V - R$, and $B - R$ values were obtained by averaging the observed colors of all measured galaxies in each group. The measured colors were corrected to zero redshift using the K values listed in table 5. The corrected colors are, to high order, independent of the redshift[1] because the K reddenings are well known for small values of the redshift $z \equiv \Delta\lambda/\lambda_0$. The colors, so corrected, are correlated with the path length through our Galaxy in figure 1. The dependence on galactic latitude is small but definite, in agreement with the prior conclusion of Peterson (1970) from different data using the same method.

Open circles in figure 1 are radio sources marked *yes* in table 4. Closed circles are the clusters and groups in tables 2 and 3. Least-squares solutions with their correlation coefficients are

$$B - V = \underset{\pm 0.006}{0.976} + \underset{\pm 0.005}{0.033}(\csc b - 1)\,; \qquad |r| = 0.56\,, \tag{1}$$

$$V - R = \underset{\pm 0.005}{0.861} + \underset{\pm 0.005}{0.026}(\csc b - 1)\,; \qquad |r| = 0.55\,, \tag{2}$$

and

$$B - R = \underset{\pm 0.009}{1.837} + \underset{\pm 0.010}{0.059}(\csc b - 1)\,; \qquad |r| = 0.62\,, \tag{3}$$

where the quoted errors are 1 sigma values.

There is no evidence from these data for a general half-layer absorption anywhere near as strong as suggested by the absorption values at the poles inferred from galaxy counts. Our data force the same dilemma as others before them: either the galaxy counts above $|b| > 30°$ have little to do with those at lower latitudes (Noonan 1971),

TABLE 5

ADOPTED K CORRECTIONS*

z	$K(B-V)$	$K(V-R)$	$K(B-R)$	K_B	K_V	K_R
0.00.....	0.00	0.00	0.00	0.00	0.00	0.00
0.04.....	0.13	0.03	0.16	0.19	0.06	0.03
0.08.....	0.27	0.05	0.32	0.40	0.13	0.08
0.12.....	0.42	0.08	0.50	0.62	0.20	0.12
0.16.....	0.55	0.11	0.66	0.82	0.27	0.16
0.20.....	0.64	0.17	0.81	1.03	0.39	0.22
0.24.....	0.69	0.26	0.95	1.22	0.53	0.27
0.28.....	0.71	0.39	1.10	1.40	0.70	0.31
0.32.....	...	0.53	...	...	0.88	0.35
0.36.....	...	0.68	...	...	1.08	0.40
0.40.....	...	0.77	...	...	1.25	0.48
0.44.....	...	0.84	...	...	1.41	0.57
0.48.....	...	0.88	...	...	1.54	0.66

*Combination of Whitford and Schild and Oke's values in Ap. J. 169, 209 and 215, 1971.

[1] Deviations from table 5 due to color evolution in the look-back time will not affect the problem discussed here because most of the galaxies that enter the latitude dependence have redshifts smaller than $z \simeq 0.16$, where the time variation of color is clearly negligible by the results of later sections.

or the ratio of absorption to reddening is very large. The present data shed no light on the alternatives, but the result of Freeman (1973) for the highly obscured galaxy Lyngå 1 show that a high ratio is inadmissible. McClure and Crawford's (1971) model gives an acceptable solution.

The ratio of the latitude coefficients in equations (1) and (2) is 1.27. Although this number has appreciable error due to the high scatter of figure 1, it is the same as the ratio of reddenings for normal galactic dust of $E(B - V)/E(V - R) = 1.25$ from Whitford (1958) and Nandy (1964, table 13). This satisfactory agreement leads us to believe that the correlations in figure 1 actually represent true reddening.

In view of these results, we have reconsidered the absorption corrections of Paper II (§ III*b*), and adopt the following modified equations to be used in the next several papers of the series:

$$\begin{aligned} A_B &= 0.132(\csc b - 1) \qquad \text{for } |b| \leq 50^\circ\,, \\ A_B &= 0 \qquad\qquad\qquad\qquad \text{for } |b| \geq 50^\circ\,, \end{aligned} \tag{4}$$

but with equation (4) modified slightly between $|b| = 40°$ and 50° so that the approach to zero at 50° is smooth with no discontinuity:

$$A_V = 0.75 A_B\,, \qquad A_R = 0.72 A_V\,. \tag{5}$$

V. DETERMINATION OF REDSHIFTS FROM COLORS ALONE

The observed mean colors were corrected for latitude effect by equations (1)–(3) and are listed in columns (4), (6), and (8) of table 6. Colors in these columns should then depend only on the intrinsic properties of the galaxies themselves, and a function of redshift alone.

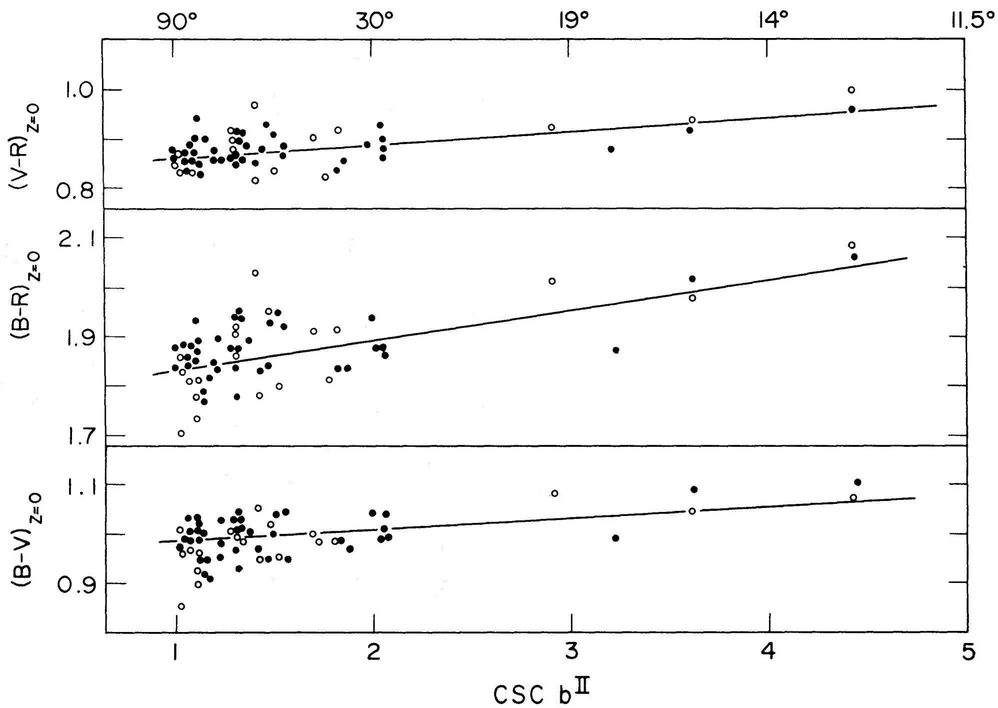

FIG. 1.—Correlation of colors, corrected to zero redshift, with path length through the galaxy. *Closed circles*, clusters and groups from tables 2 and 3. *Open circles*, radio galaxies in which the effect of emission lines on their colors is small or negligible.

TABLE 6

CORRECTED COLORS FOR CLUSTERS, GROUPS, AND RADIO GALAXIES

Object (1)	b (2)	z (3)	$\langle B-V\rangle$ $-E$ (4)	$\langle B-V\rangle$ $-E-K$ (5)	$\langle V-R\rangle$ $-E$ (6)	$\langle V-R\rangle$ $-E-K$ (7)	$\langle B-R\rangle$ $-E$ (8)	$\langle B-R\rangle$ $-E-K$ (9)	Galaxies
				Clusters					
Virgo........	+70	0.00381	1.028	1.028	0.848	0.848	1.876	1.876	N4486
Peg I........	-48	0.01279	1.066	1.036	0.894	0.884	1.960	1.920	N7619, 7626, 7562
0122 + 3305...	-29	0.0170	1.020	0.970	0.847	0.837	1.867	1.807	N507, 499, 508
Per (N1265) ..	-13	0.0181	1.036	0.986	0.880	0.860	1.916	1.846	N1265 (poor obs)
A1213........	+69	0.0287	1.093	1.003	0.853	0.833	1.946	1.836	N1, N2
A119.........	-64	0.0387	1.124	1.004	0.880	0.850	2.004	1.854	N1, N2
Peg II	-48	0.0428	1.162	1.022	0.937	0.897	2.099	1.919	N7501, 7503
2322 + 1425...	-43	0.0439	1.078	0.938	0.906	0.866	1.984	1.804	N7649, N1, N7
0106 - 1536...	-78	0.0526	1.149	0.979	0.896	0.856	2.045	1.835	N1, N2, N10
1239 + 1852...	+81	0.0718	1.247	1.007	0.922	0.872	2.169	1.879	N1, N2, N4
1520 + 2754...	+57	0.0722	1.150	0.910	0.944	0.894	2.094	1.804	N2, N3
A2670........	-69	0.0774	1.244	0.984	0.920	0.860	2.164	1.844	N1, NA
A2029........	+50	0.0777	1.220	0.960	0.912	0.852	2.132	1.812	N1
0705 + 3506...	+18	0.0779	1.176	0.916	0.872	0.812	2.048	1.728	N1, N2, N1A
1513 + 0433...	+49	0.0944	1.239	0.919	0.897	0.837	2.136	1.756	N1
A98..........	-42	0.1028	1.344	0.984	0.978	0.908	2.322	1.892	N1, NA, NE
A274.........	-64	0.1289	1.434	0.984	0.985	0.895	2.419	1.879	N1, NA, NE
0025 + 2223...	-40	0.1594	1.480	0.930	0.980	0.860	2.460	1.790	N1, N2, N4
0138 + 1832...	+61	0.1917	1.560	0.940	1.106	0.946	2.666	1.886	N1, N1A
0855 + 0327...	+29	0.2018	1.644	1.004	1.064	0.894	2.708	1.898	N1, N2, N2A, N5
1447 + 2617...	+63	0.36	1.486	...	1.597	...	3.083	...	N4
3C295........	+61	0.461	1.415	...	1.731	...	3.146	...	N1
				HMS Groups					
G68..........	-32	0.0226	1.011	0.941	0.855	0.835	1.866	1.776	N68, 70, 71
G80..........	-40	0.0209	1.090	1.030	0.876	0.856	1.966	1.886	N80, 83
G128.........	-60	0.0155	0.955	0.915	0.859	0.839	1.814	1.754	N128
G194.........	-60	0.0177	0.990	0.940	0.854	0.834	1.844	1.774	N193, 194
G383.........	-30	0.0175	1.062	1.012	0.879	0.859	1.941	1.871	N383
G507.........	-29	0.0155	1.005	0.965	0.853	0.833	1.858	1.798	N507, 499, 508
G547.........	-63	0.0180	1.050	1.000	0.881	0.861	1.931	1.861	N547, 545, 543, 564
G741.........	-54	0.0188	1.072	1.022	0.854	0.874	1.946	1.876	N741
G1600........	-33	0.0160	1.012	0.962	0.834	0.814	1.846	1.776	N1600
G2563........	+29	0.0159	1.007	0.957	0.872	0.852	1.879	1.809	N2562, 2563
G2832........	+44	0.0200	1.022	0.962	0.859	0.839	1.881	1.801	N2832, 2831
G3158........	+55	0.0234	1.019	0.949	0.885	0.865	1.904	1.814	N3158, 3159, 3163
G3193........	+55	0.0040	0.973	0.973	0.849	0.849	1.822	1.822	N3193
Leo..........	+64	0.0026	1.030	1.030	0.889	0.889	1.919	1.919	N3368, 3379
G5044........	+46	0.0087	1.021	0.991	0.880	0.870	1.901	1.861	N5044
G5077........	+50	0.0084	1.034	1.004	0.858	0.848	1.892	1.852	N5077
G5371........	+71	0.0076	1.007	0.987	0.866	0.856	1.873	1.843	N5353, 5354
G5846........	+49	0.0060	1.024	1.004	0.858	0.848	1.882	1.852	N5846, 5813, 5831
G7242........	-16	0.0204	1.070	1.000	0.868	0.848	1.938	1.848	N7242
G7385........	-41	0.0258	1.103	1.023	0.916	0.886	2.019	1.909	N7385, 7386
G7619........	-48	0.0128	1.058	1.018	0.907	0.897	1.965	1.915	N7619, 7626, 7562
VV172	+45	0.0526	1.136	0.966	0.931	0.891	2.067	1.857	A, C, D, E
				Radio Sources With $S_6 \leq 4$					
									S_6
3C15.........	-64	0.0733	1.146	0.896	0.887	0.827	2.033	1.723	~ 1
3C29.........	-64	0.0450	1.059	0.919	0.890	0.850	1.949	1.769	0
3C76.1.......	-36	0.0328	1.082	0.982	0.912	0.882	1.994	1.864	0
3C78.........	-45	0.0289	1.134	1.044	0.973	0.953	2.107	1.997	1:
3C88.........	-42	0.0302	1.104	1.004	0.938	0.908	2.042	1.912	2
3C264........	+73	0.0206	1.023	0.963	0.879	0.859	1.902	1.822	0
3C270........	+67	0.0070	0.990	0.970	0.838	0.828	1.828	1.798	0
3C272.1......	+74	0.0029	1.022	1.012	0.842	0.842	1.864	1.854	< 3
3C278........	+50	0.0143	1.040	1.000	0.884	0.874	1.924	1.874	0
3C293........	+76	0.0454	0.990	0.850	0.879	0.839	1.869	1.689	~ 2
3C296........	+62	0.0237	1.031	0.961	0.857	0.837	1.888	1.798	0
3C317........	+50	0.0351	1.095	0.985	0.912	0.872	2.007	1.857	3
3C318.1......	+49	0.0457	1.121	0.981	0.942	0.902	2.063	1.833	0
3C338........	+44	0.0303	1.046	0.946	0.832	0.802	1.878	1.748	0
3C388........	+20	0.0917	1.335	1.024	0.925	0.865	2.260	1.889	1
3C402........	+13	0.0259	1.042	0.962	0.925	0.905	1.967	1.867	0
3C442........	-34	0.0270	1.038	0.958	0.832	0.802	1.870	1.760	~ 1
3C449........	-16	0.0181	1.010	0.960	0.855	0.835	1.865	1.795	0
3C455........	-41	0.0331	1.040	0.940	0.853	0.823	1.893	1.763	0
3C465........	-33	0.0301	1.060	0.960	0.914	0.894	1.974	1.854	1
				Radio Sources With $S_6 > 4$					
3C17.........	-65	0.2201	0.752	0.082	0.852	0.642	1.604	0.724	7
3C26.........	-67	0.2106	1.137	0.487	0.858	0.668	1.995	1.155	11
3C28.........	-37	0.1959	1.390	0.760	1.128	0.968	2.518	1.728	2
3C33.........	-49	0.0600	1.152	0.952	0.835	0.785	1.987	1.737	12
3C66.........	-17	0.0215	0.943	0.883	0.832	0.812	1.775	1.695	?
3C75.........	-45	0.0241	1.213	1.133	1.022	1.002	2.235	2.135	?
3C98.........	-31	0.0306	1.171	1.071	0.948	0.918	2.119	1.989	8
3C192........	+26	0.0596	1.163	0.963	0.832	0.782	1.995	1.745	~ 5?
3C198........	+23	0.0809	0.849	0.578	0.749	0.689	1.598	1.267	7
3C219........	+45	0.1745	1.469	0.889	0.929	0.799	2.398	1.688	8
3C223.1......	+49	0.1075	1.279	0.909	0.912	0.832	2.191	1.741	~ 6:
3C381........	+23	0.1614	1.369	0.818	0.884	0.764	2.253	1.582	> 8
3C382........	+17	0.0586	1.063	0.873	0.867	0.817	1.930	1.690	5
3C436........	-19	0.2154	1.382	0.722	1.116	0.916	2.498	1.638	5
3C452........	-17	0.0820	1.215	0.935	0.862	0.802	2.077	1.737	5
3C456........	-46	0.2337	0.777	0.097	1.125	0.885	1.902	0.982	7:
MSH 23-112 ..	-64	0.0825	1.049	0.769	0.934	0.874	1.983	1.643	7

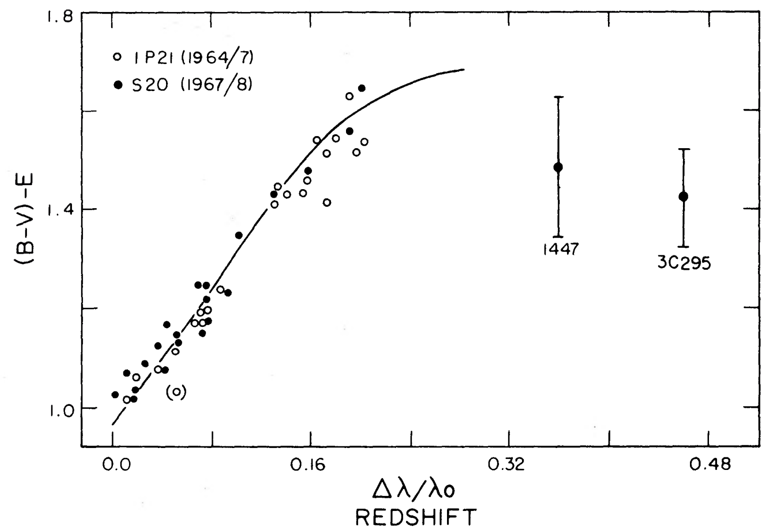

FIG. 2.—Correlation of the $B - V$ color, corrected for galactic reddening by eq. (1), with redshift for groups and clusters from tables 2 and 3. *Closed circles*, the present S20 photometry; *open circles*, independent S4 photometry reported in Paper II. The line is the calculated relation obtained by shifting the standard energy distribution of giant E galaxies through the measuring bands.

The color-redshift effect in $B - V$ is shown in figure 2. Closed circles are the present data, open circles are the similarly re-reduced colors from Paper II (table 1) discussed by Oke and Sandage (1968), but there without latitude correction.

A small difference exists between the open and closed circles for $z \gtrsim 0.16$: the S4 colors are slightly bluer than the S20 values. Comparison of the overlap between the S20 data in tables 2, 3, and 4 here with the 1P21 data of Papers II and III give $\langle\Delta(B - V)\rangle = 0.016 \pm 0.006$ (rms) in the sense of the S4 photometry minus this paper. The sigma of the distribution of color differences between the two sets is $\sigma = 0.038$ mag. If equal errors are present in both investigations, each will have a distribution of internal errors of $\sigma E(B - V) \simeq 0.027$ mag.[2] The source of the slight systematic difference between the open and the closed dots at $z \equiv \Delta\lambda/\lambda_0 \simeq 0.16$ in figure 2 is not known.

The solid line in figure 2 is the predicted run of color with redshift if all E and S0 galaxies have an identical spectrum equal to the mean of the standard galaxy of Whitford (1971) and Schild and Oke (1971). These calculated $K(B - V)$ values are listed in table 5. The curve has been normalized to $(B - V)_0 = 0.97$ at $z = 0$, which is that calculated by Schild and Oke from their energy distribution, using the precepts of Matthews and Sandage (1963). The earlier calculation by Oke and Sandage (1968) gave $B - V = 1.04$ for the centralmost region of M31 alone ($\theta \simeq 14$ arc sec diameter). This was redder than the present value by 0.07 mag due to the radial color gradient, which explains entirely the color shift of 0.07 mag required by these authors to make their calculations coincide with the present observations in zero point.

It is evident from figure 2 that the $B - V$ colors become bluer again as the redshift becomes larger than $z \simeq 0.3$. The behavior is expected because the ultraviolet energy

[2] This, then, is not particularly good photometry judged against what can be routinely achieved for stars. The large dispersion is undoubtedly due to the addition of the color data from Mount Wilson, where the sky is not dark. The uncertainty is due to the large coincidence correction as previously discussed. In view of the importance of the color distribution discussed in § VII, the present data should be repeated using the modern wide-bandwidth (33 MHz) preamplifiers, now in use, that reduce the dead-time correction to negligible values.

distribution flattens shortward of $\lambda_0 \simeq 3600$ Å relative to its precipitous drop in the range 3600 Å $< \lambda <$ 4200 Å. The B and V filters fall in this region of changing gradient in the proper galaxy spectrum if the redshift is larger than $z \simeq 0.3$. The bluing occurs in $B - V$ at this redshift for the same reason that $U - B$ becomes bluer for increasing redshift in the interval $0 < z \lesssim 0.04$ (Sandage 1972*b*, table 3).

Figure 3 shows the color-redshift effect in $V - R$, again compared with the predicted variation. The agreement is good. The zero-point of the line has been put at $(V - R)_0 = 0.86$, which is the empirical value for $z = 0$. The main point to note in figure 3 is the shallow gradient for redshifts smaller than ~ 0.16, and the rapid steepening thereafter. Note also that the shape of the curve for $z \gtrsim 0.22$ is similar to that in figure 2 for $z \geq 0$ as expected because the proper wavelengths of the B and V filters at $z = 0$ are nearly the same as those for the V and R filters for $z \simeq 0.2$.

An important practical application of these color-redshift effects is evident from figure 3. The variation of color with z is well enough defined, and is steep enough in the interesting region beyond $z \gtrsim 0.2$ that moderately accurate redshifts can be determined from the $V - R$ broad-band colors alone. From the horizontal scatter in this diagram, and from figure 4 for $B - R$, the error for such measurements will be of order $\sigma(\Delta z) \simeq 0.01$, which is highly satisfactory for many purposes. The technique is the same as used by Baum (1962) except that it can evidently be simplified to two, or at most three, colors, for $z \lesssim 0.5$.

The information in figures 2–4 allows us to optimize a broad-band system for the problem. The diagrams show that (1) $\Delta(B - V)$ is most sensitive to redshift in the low-z range $0 < z \lesssim 0.2$; it becomes insensitive and multivalued for larger z. (2) $\Delta(V - R)$ is sensitive to redshift in the range $0.2 \leq z \lesssim 0.6$; it becomes insensitive and multivalued for larger z for the same reason as $B - V$. (3) For redshifts larger than $z = 0.6$, and in the absence of strong color-evolution in the look-back time, a band near $\langle\lambda\rangle = 8500$ Å, combined with R will reproduce the crucial steep part of the curves in figures 2 and 3 in the redshift range $0.9 > z \gtrsim 0.6$.

Redshifts by color can therefore be obtained in the range $0.2 < z \lesssim 0.9$ *by combining measurements made at* $\langle\lambda\rangle \simeq 5500$ Å, 6700 Å, *and* 8500 Å *only. To cover the entire range* $0 < z \lesssim 0.9$ *requires only the addition of the B filter near* $\langle\lambda\rangle \simeq 4400$ Å.

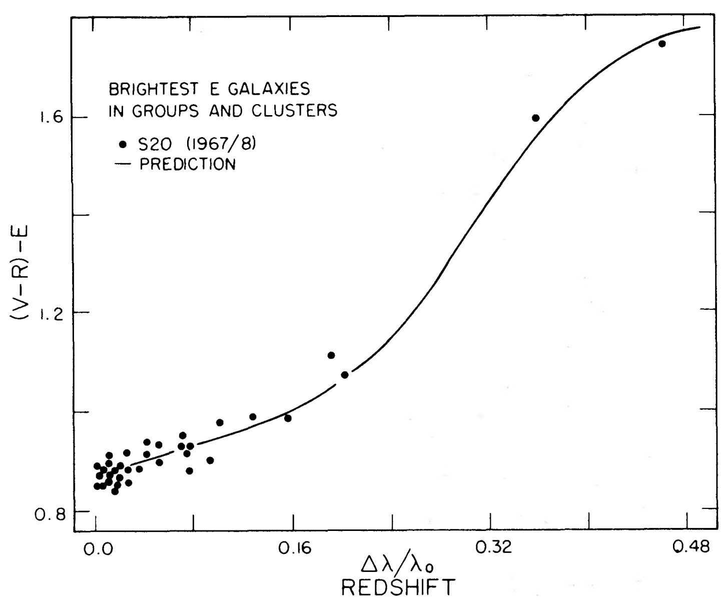

FIG. 3.—Same as fig. 2 for reddening corrected $V - R$ colors

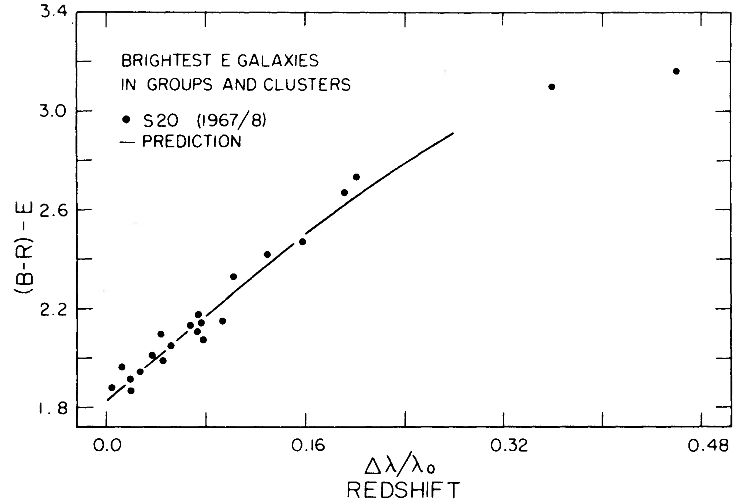

FIG. 4.—Same as fig. 2 for reddening corrected $B - R$ colors

These color properties of E and S0 galaxies are the basis upon which a redshift program for faint clusters has been started by Kristian, Westphal, and the writer using a silicon vidicon area photometer similar to that developed by McCord and Westphal (1972).

The similarity of the energy distributions of the galaxies in the sample is shown in figure 5, which is the histogram of measured colors corrected for galactic and K reddening. The rms spread is $\sigma \simeq 0.03$ mag for $V - R$, and $\sigma \simeq 0.04$ mag for $B - V$. The external errors in the photometry, estimated earlier in this section, are distributed with $\sigma_E \simeq 0.027$ mag, giving a true cosmic dispersion in $B - V$ of $\sigma(B - V) \simeq 0.029$ mag. The homogeneity of the colors for giant E and S0 galaxies implied by this small spread confirms earlier work of Stebbins and Whitford (1937, 1952) where the similarity was first demonstrated, by Lasker (1966), Oke and Sandage (1968), and others.

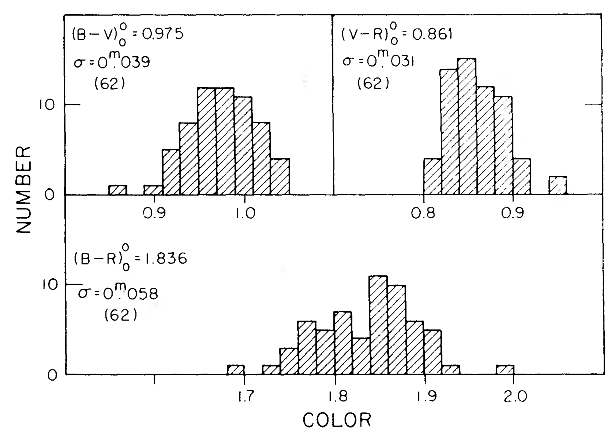

FIG. 5.—Distribution of observed colors for the galaxies in clusters, groups, and radio sources with $S_6 \leq 4$ that are listed in table 6.

VI. LIMITS ON COLOR EVOLUTION IN THE LOOK-BACK TIME

The generally good agreement of the predictions with the observations in figures 2, 3, and 4 precludes any gross color evolution in the look-back time. The same conclusion follows from the recent observation of 3C 295 with higher spectral resolution (Oke 1971). But some color evolution must, of course, occur, and it is of interest to put observational limits on the effect, and to estimate reasonable expectation values from current knowledge of stellar evolution.

Empirical data are available on the correlation of integrated colors and age for *simple* stellar aggregates such as star clusters, where the cluster members are nearly coeval (Sandage 1963, fig. 7; Gray 1965, fig. 4). In the age range that is relevant here, $8 < \log t \lesssim 10$ where t is in years, the color rate from both quoted studies is $\Delta(B - V)/\Delta \log t \simeq 0.3$ mag per factor of 10 in age, i.e., 0.3 mag dex^{-1}. The stated time interval covers the range of main-sequence termination points from about 1 mag brighter than M11 at $M_V \simeq -2$ to NGC 188 at $M_V \simeq +4$ (see, for example, the composite C-M diagram of Sandage and Eggen 1969, fig. 6). The colors of the termination point itself vary between $(B - V)_0 = -0.1$ and $(B - V)_0 = +0.6$ over the stated time interval, and the colors of the integrated aggregates change from $+0.2$ to $+0.8$, according to the color-age correlations previously cited.

But it is expected that E and S0 galaxies will show smaller color variations because more light is locked in the unevolved faint main sequence. However, the variation clearly cannot be zero because the main-sequence termination point will have changed by *6 magnitudes* in V, and 0.6 mag in $B - V$, for the factor of 100 in age. In the following we carry through two calculations based on color-evolutionary rates of 0.3 mag dex^{-1} and 0.1 mag dex^{-1}, which seem likely to bracket the true range.

Consider first the bulk of the points in figures 2 and 3. What is the expected color change at $z = 0.2$ for the two rates? Let the age of the oldest galaxies be 13×10^9 years. For $q_0 = 0$, the look-back time is $t_{\rm LB} = [z/(1 + z)]H_0^{-1}$ which, for $z = 0.2$ and $H_0 = 55$ (Sandage and Tammann 1973) is $t_{\rm LB} = 3 \times 10^9$ years. The time is essentially the same at 2.7×10^9 years if $q_0 = +1$ (Sandage 1961, table 3). Therefore, the ratio of the age of galaxies observed at a redshift of 0.2 to that of galaxies seen nearby is $(13 - 3)/13$ or $\Delta \log t = 0.11$. Hence, the expected color change in proper wavelengths will be $\Delta(B - V) = 0.03$ mag for the rate of 0.3 mag dex^{-1}, and $\Delta(B - V) = 0.01$ mag for the smaller rate of 0.1 mag dex^{-1}. Both predictions are compatible with the observations, which show no systematic color difference among galaxies as a function of redshift at the 0.05 mag level[3] for $0 \leq z \leq 0.2$.

For 3C 295 at $z = 0.461$, the look-back time for $q_0 = 0$ is 5.6×10^9 years, or the age is $(13 - 5.6) \times 10^9 = 7.4 \times 10^9$ years, or $\Delta \log t = 0.24$. In this time interval the expected color changes are $\Delta(B - V) = 0.07$ mag for the 0.3 mag dex^{-1} rate, and 0.02 mag for the slower rate. Oke's (1971) observations may just preclude the 0.07 mag rate, but do not at all eliminate the smaller rate.

Constraints put by the present observations on the color evolution are therefore not severe and do not yet positively eliminate even the fast rates predicted from open clusters. The estimated rates are, however, fast enough so that they can be seriously looked for observationally at $z > 0.4$, and detailed scanner observations are clearly the way to do it.

The main conclusion from this section is that color-evolutionary rates as high as $\Delta(B - V)/\Delta \log t = 0.2$ mag dex^{-1} would be undetected for $z \leq 0.4$ in any data now available. Very slow rates such as $\Delta(B - V)/\Delta \log t \lesssim 0.05$ mag dex^{-1} appear to be unrealistic from considerations of the stellar content of E galaxies in terms of a composite C-M diagram.

[3] It should be noted that the observations are not made at the proper wavelengths (in the rest frame of the galaxies). However, figures 2 and 3 together, which for various z-values bracket $B - V$ (proper), show that no color evolution in $B - V$(proper) exists larger than the stated limits.

VII. THEORETICAL COLOR DISTRIBUTIONS FOR VARIOUS WORLD MODELS COMPARED WITH OBSERVATIONS

a) *Steady-State Prediction*

On a steady-state hypothesis, all structures must be renewed continuously (statistically uniformly) in time, and any sufficiently large region of space will contain galaxies of all ages. However, the probability of finding an extremely old galaxy is small because the expansion will remove most such systems out of the volume. McCrea (1950) has given the distribution of ages such that $f(t)dt$ is the number of galaxies whose ages are between t and $t + dt$, by considering a uniform production rate and removal by expansion. With assumptions on the color change with time, $f(t)$ can be transformed into the distribution $g(B - V)$ per unit $B - V$ interval.

McCrea shows that

$$f(t)dt = 3nH \exp(-3Ht)dt\,, \tag{6}$$

where H is the expansion rate and n is the number of galaxies in the sample. Over the time interval discussed in the last section, the color change with time will be closely approximated by

$$B - V = a \log t + b\,, \tag{7}$$

which gives t for any $B - V$ once a and b are known.

Equation (6) can be transformed into the distribution of colors by differentiating equation (7) and substituting into equation (6) giving

$$g(B - V)\Delta(B - V) = 6.91na^{-1}Ht \exp(-3Ht)\Delta(B - V)\,, \tag{8}$$

which, parametrically with equation (7), is a function of $B - V$ alone.

Is equation (8) applicable to our present sample of *cluster* galaxies? It might be argued that clusters form in the steady state only after the galaxies destined to become members are already older than a certain age, the process of clustering itself taking an appreciable time. That this is not the case is shown directly by the observations of cluster and field E galaxies themselves (McClure and van den Bergh 1968) in which the color properties of both samples are the same. Further evidence against such an argument is the similarity of colors of E galaxies in very dense clusters and in sparse groups such as G194, G5077, and G5353 in our sample, where the colors are significantly the same as for first-ranked members of the very rich clusters. This similarity of colors argues against a detectable age difference in groups of different density. Hence groups and clusters probably do not form by the slow process of accumulation, where the formation time itself would depend on the density of the aggregate.

The conclusion is that our sample of brightest galaxies in groups and clusters should not be biased toward old systems merely because they are in aggregates. Rather, the direct observations of McClure and van den Bergh show that cluster members are representative of field ellipticals.

Our observed distribution is compared with equation (8) in figure 6 for three color-evolution rates, using the color-age relations

$$B - V = 0.3 \log t - 2\,, \tag{9}$$

$$B - V = 0.1 \log t\,, \tag{10}$$

and

$$B - V = 0.05 \log t + 0.53\,. \tag{11}$$

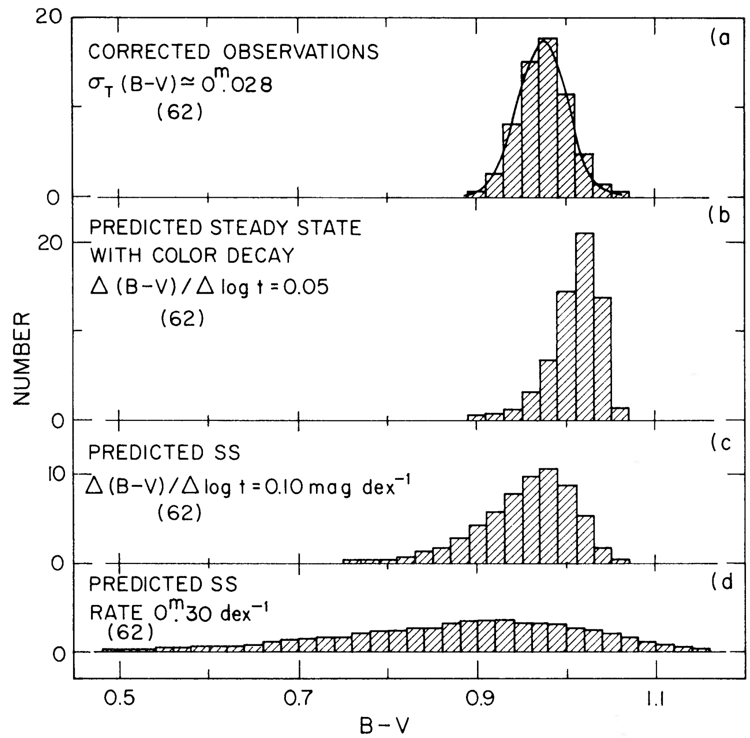

FIG. 6.—Comparison of the observed color distribution, corrected for error (*top panel*), with predictions for the steady-state model (eq. [8]) for three-color decay rates. The rate in panel (*b*) at $\Delta(B - V)/\Delta \log t = 0.05$ mag dex^{-1} is unrealistically small.

These have been normalized to give $B - V \simeq 1.04$ at $t = 13 \times 10^9$ years, in reasonable agreement with what we know of colors and ages of E galaxies deduced from data in the Local Group.

We have normalized equation (8) to $n = 62$ to compare with the observed sample in figure 5. Shown in figure 6 are the three theoretical distributions of equation (8) with equations (9)–(11), using $H_0^{-1} = 17.7 \times 10^9$ years (Sandage and Tammann 1973). The observed distribution of figure 5, corrected for the observational errors of $\sigma_E = 0.028$ mag from § V, is shown in the top panel.

The predicted distributions for the two color rates of 0.1 and 0.3 are in clear disagreement with the observations. Too many blue (young) galaxies are predicted, and the shape of the distribution is strongly non-Gaussian. The distribution for the slow rate (panel *b*) is approximately as narrow as the observations, but the required rate is too slow to be realistic. The color distributions predicted by a steady-state model appear then to disagree with observation by a wide margin.

b) *Continuous Galaxy Formation with an Upper Age Limit*

Another simple model is continuous galaxy formation within a Friedmann universe, with an upper limit to the age of the oldest galaxy. If the formation rate is constant per unit time, then, by the same argument that transformed equation (6) to equation (8), it follows that the expected color distribution is

$$g(B - V)\Delta(B - V) = 2.303 nta^{-1}T_0^{-1}\Delta(B - V)\,, \tag{12}$$

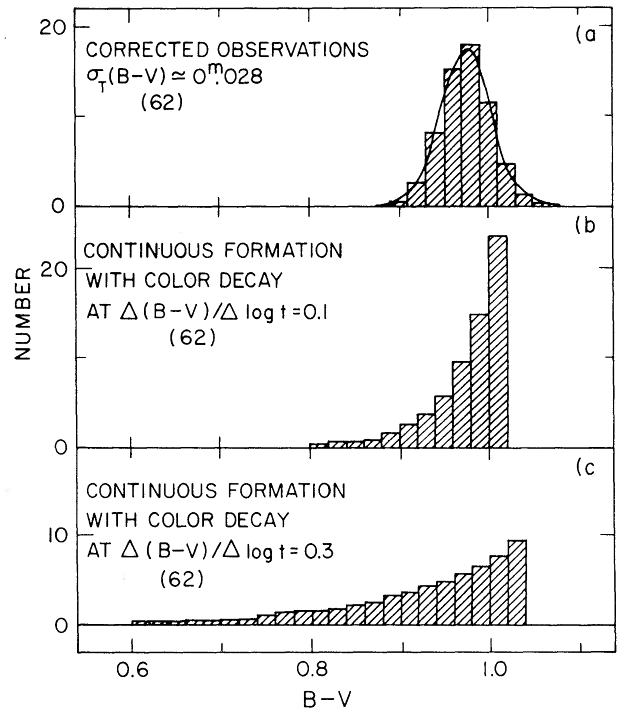

FIG. 7.—Same as fig. 6 but for a model with a uniform E galaxy formation rate with time, and with an upper limit to the age of the oldest galaxy at 13×10^9 years.

where T_0 is the maximum age, and a and t are given by equation (7), or the explicit forms of equations (9) and (10). Equation (12) is a rising exponential in $B - V$, as seen by eliminating t using equation (7).

The two predicted distributions are shown in figure 7 using equations (9) and (10) with $T_0 = 13 \times 10^9$ years and a lower age limit of 10^8 years. Comparison with the observations given in the top panel shows that neither prediction agrees well with observation. From this we would conclude that the formation of giant E and S0 galaxies took place during a shorter time interval than $9 < \log t < 10$. This is the main result of the present paper. It agrees with the formation history that is required by the distribution of flattenings of elliptical galaxies (Sandage, Freeman, and Stokes 1970), where such galaxies must presumably form during the short time interval of about a free-fall time (generally less than 10^9 years) by collapse from the pregalactic medium.

c) *Bias*

The preceding arguments depend on two assumptions:

1. Ages of E and S0 galaxies in clusters and groups are representative of the E galaxy population as a whole (§ VII*a*).

2. There has been no bias that has caused us to observe galaxies in a restricted age range only, rather than in the total relevant range. The only criterion used to choose the galaxies in tables 2 and 3 was that the aggregates must contain mostly E galaxies, not spirals. Bias would be present due to this section only if ellipticals were of systematically different age than spirals, such as would obtain if, say, ellipticals evolved from spirals, causing the early end of the age sequence to be eliminated artificially from the sample. However, that spirals and ellipticals are not connected evolutionarily is shown by the strong dichotomy in the flattenings (Hubble 1926; de Vaucouleurs 1959;

Sandage *et al.* 1970). And because color was not used as a selection criterion for tables 2–4, there should be no age bias.

The conclusions from figures 6 and 7 are then (1) the absence of blue giant ellipticals is real; (2) no young (i.e., $t \lesssim 10^9$ years) giant E galaxies exist in our sample.[4] Whether they exist in any sample requires more extensive data, but figures 6 and 7 show that such galaxies do not exist in the numbers required, either by the steady-state or by the continuous-production models. Our present data are consistent with the view that E galaxies are the same age to within close limits, that they formed at some definite time in the past, and that no substantial fraction of the class, if any, has formed more recently. It will be possible to put closer limits on the interval of galaxy birth when color observations of giant E galaxies are available that are accurate to 1 percent or better.

It is a pleasure to thank personnel of the Astroelectronics Laboratory for providing the pulse-counting equipment and the data readout systems on both Mount Wilson and Palomar. Larry Blakeé and Martin Olsiewski were especially helpful in the electronic setups. The data could not have been obtained without the cheerful help of the night assistants E. Hancock at the 100-inch, and G. Tuton and J. Carrasco at Palomar. It is a particular pleasure to thank them.

The paper was organized in Australia, and I wish to acknowledge the kind hospitality of O. J. Eggen at Mount Stromlo Observatory, and to thank the Australian-American Educational Foundation for the award of a Fulbright-Hays Scholarship that made the trip possible.

Finally, I wish to thank with special appreciation W. L. W. Sargent for permitting me to use and to quote his redshift measurements for the Abell clusters 98, 274, 655, 2029, 2224, and 2670 before his publication of them.

REFERENCES

Baum, W. A. 1959, *Pub. A.S.P.*, **71**, 118.
———. 1962, in *Problems of Extragalactic Research*, ed. G. C. McVittie (New York: Macmillan), p. 390.
Bautz, L., and Morgan, W. W. 1970, *Ap. J. (Letters)*, **162**, L149.
Eggen, O. J., and Sandage, A. 1964, *Ap. J.*, **140**, 130.
———. 1969, *ibid.*, **158**, 6.
Feige, J. 1959, *Ap. J.*, **129**, 600.
Freeman, K. C. 1973, *Ap. J.*, in press.
Gray, D. F. 1965, *A.J.*, **70**, 362.
Hubble, E. 1926, *Ap. J.*, **67**, 321.
———. 1934, *ibid.*, **79**, 8.
Humason, M. L., Mayall, N. U., and Sandage, A. 1956, *A.J.*, **61**, 97.
Iriarte, B., Johnson, H. L., Mitchell, R. I., and Wisniewski, W. Z. 1965, *Sky and Tel.*, **30**, 21.
Johnson, H. L., and Harris, D. L. 1954, *Ap. J.*, **120**, 196.
Johnson, H. L., Mitchell, R. I., Iriarte, B., and Wisniewski, W. Z. 1966, *Comm. Lunar and Planetary Lab.*, **4**, No. 63.
Johnson, H. L., and Morgan, W. W. 1953, *Ap. J.*, **117**, 313.
Johnson, H. L., and Sandage, A. 1955, *Ap. J.*, **121**, 616.
Lasker, B. M. 1966, *A.J.*, **71**, 862.
Luyten, W. J. 1949, *Ap. J.*, **109**, 528.
McClure, R. D., and Bergh, S. van den. 1968, *A.J.*, **73**, 1008.
McClure, R. D., and Crawford, D. L. 1971, *A.J.*, **76**, 31.
McCord, T. B., and Westphal, J. A. 1972, *Appl. Optics.*, **11**, 522.
McCrea, W. H. 1950, *Endeavour*, **9**, 3.
Matthews, T. A., Morgan, W. W., and Schmidt, M. 1964, *Ap. J.*, **140**, 35.
Matthews, T. A., and Sandage, A. 1963, *Ap. J.*, **138**, 30.
Mendoza, E. E. 1967, *Bol. Obs. Tonantzintla y Tacubaya*, **4**, 149.
Nandy, K. 1964, *Pub. Roy. Obs. Edinburgh*, **3**, No. 6.

[4] To be sure, blue E galaxies do exist, provided that they are of faint absolute magnitude, but they are blue for reasons other than age (Baum 1959; Sandage 1972*b*).

Noonan, T. W. 1971, *A.J.*, **76**, 190.
Oke, J. B. 1971, *Ap. J.*, **170**, 193.
Oke, J. B., and Sandage, A. 1968, *Ap. J.*, **154**, 21.
Penston, M. J., Penston, M. V., and Sandage, A. 1971, *Pub. A.S.P.*, **83**, 783.
Peterson, B. A. 1970, *A.J.*, **75**, 695.
Sandage, A. 1953, *A.J.*, **58**, 61.
———. 1958, *Ap. J.*, **128**, 150.
———. 1961, *ibid.*, **134**, 916.
———. 1963, *ibid.*, **138**, 863.
———. 1970, *ibid.*, **162**, 841.
———. 1972*a*, *ibid.*, **173**, 485 (Paper I).
———. 1972*b*, *ibid.*, **176**, 21.
———. 1972*c*, *ibid.*, **178**, 1 (Paper II).
———. 1972*d*, *ibid.*, **178**, 25 (Paper III).
Sandage, A., and Eggen, O. J. 1969, *Ap. J.*, **158**, 685.
Sandage, A., Freeman, K. C., and Stokes, N. R. 1970, *Ap. J.*, **160**, 831.
Sandage, A., and Smith, L. L. 1963, *Ap. J.*, **137**, 1057.
Sandage, A., and Tammann, G. A. 1973, in preparation.
Sandage, A., and Walker, M. F. 1966, *Ap. J.*, **143**, 313.
Schild, R., and Oke, J. B. 1971, *Ap. J.*, **169**, 209.
Schmidt, M. 1965, *Ap. J.*, **141**, 1.
Shane, C. D., and Wirtanen, C. A. 1954, *A.J.*, **59**, 285.
———. 1967, *Lick Obs. Bull.*, **22**, 1.
Stebbins, J., and Whitford, A. E. 1937, *Ap. J.*, **86**, 247.
———. 1952, *ibid.*, **115**, 284.
Vaucouleurs, G. de. 1959, in *Handbuch der Physik*, Vol. **53**, p. 275.
Vaucouleurs, G. de, and Malik, G. M. 1969, *M.N.R.A.S.*, **142**, 387.
Whitford, A. E. 1954, *Ap. J.*, **120**, 599.
———. 1958, *A.J.*, **63**, 201.
———. 1971, *Ap. J.*, **169**, 215.